ELSEVIER

Journal of Non-Crystalline Solids 297 (2002) 113–119

JOURNAL OF NON-CRYSTALLINE SOLIDS

www.elsevier.com/locate/jnoncrysol

Room-temperature hole-burning and sublinear hole-growth dynamics in an Sm^{2+}-doped aluminosilicate glass

Hongwei Song [a,b,*], Masayuki Nogami [b]

[a] *Laboratory of Excited State Processes, Institute of Optics, Fine Machine and Physics, Chinese Academy of Sciences, Changchun 130021, People's Republic of China*

[b] *Department of Materials Science and Engineering, Nagoya Institute of Technology, Showa, Nagoya 466-8555, Japan*

Received 12 December 2000; received in revised form 25 October 2001

Abstract

Aluminosilicate glasses doped with Sm^{2+}-ion can exhibit hole-burning at room temperature. In this paper, we investigate the hole-growth dynamics of Sm^{2+}-ion-doped aluminosilicate glasses prepared by the sol–gel method to reveal the hole-formation at room temperature. We found that the spectral holes exhibit Lorenz profiles. Hole-growth dynamics can be well fitted by the function $H(t) = \alpha t^{\beta}$. The hole-growth rate K_t decreases with hole-burning time and is proportional to the laser power of the hole-burning light. We assume that an Sm^{2+} ion and a trap nearby consist of a two-level-system (TLS). For some of the Sm^{2+} ions, the distance between the Sm^{2+} ion and the nearest trap is beyond the interaction range of tunneling in the glass network. © 2002 Published by Elsevier Science B.V.

PACS: 42.70.Ce; 81.05.Kf; 81.20.Fw; 71.20.Eh; 78.55.Hx; 42.62.Fi

1. Introduction

In recent years, persistent spectral hole-burning (PSHB) has been extensively studied in various materials because of the possibility of its application to high-density frequency domain optical storage (FDOS) [1]. Realization of room-temperature PSHB is important for recent research work [2–4]. In the family of room-temperature PSHB materials, Sm^{2+}-ions doped in various inorganic glasses are thought to be more favorable because of their wide inhomogeneous line width, compositional variety, and easy mass production [5]. So far, conventional glass melting and a sol–gel method both have been used to prepare Sm^{2+}-ion-doped glasses. Hirao et al. [6] and Izumitani and Payne melted Sm^{2+}-doped fluoride and borate glasses under a reducing atmosphere [6,7]. On the other hand, Nogami et al. [8,9] successfully prepared Sm^{2+}-doped aluminosilicate glasses by the sol–gel method. Very recently, room-temperature PSHB was also realized in Eu^{3+}-doped melt-prepared silicate glasses [10].

To develop new materials with the properties required for optical memory devices, it is important to better understand the formation mechanism of PSHB. Nogami et al. [11–14] concentrated

* Corresponding author. Tel.: +8-64 3159 37563; fax: +8-64 3159 37615.

E-mail address: songhw67@sina.com.cn (H. Song).

0022-3093/02/$ - see front matter © 2002 Published by Elsevier Science B.V.
PII: S0022-3093(01)01035-3

on understanding the mechanism of PSHB of Eu^{3+}- and Sm^{2+}-doped glasses prepared by the sol–gel method. They found that the PSHB efficiency at low temperature is proportional to the OH bond concentration in the glasses and thus the formation of PSHB was attributed to the optically activated rearrangement of OH bonds surrounding Sm^{2+}- or Eu^{3+}-ions. Previously we systematically studied the PSHB of the Sm^{2+}-ion as a function of temperature and Al_2O_3 concentration, and the thermal and light-induced hole refilling in the aluminosilicate glasses. We further found that the PSHB formation mechanism varied depending on temperature [15,16]. A hole was formed mainly by the rearrangement of OH bonds surrounding Sm^{2+}-ions at low temperature, which disappeared above 200 K because of the small barrier height between the burnt and unburnt states. On the other hand, a hole was formed by the photoionization from Sm^{2+} to Sm^{3+} through tunneling at high temperature. The traps that capture the electrons may be related to Al ions, because we found that hole-burning efficiency increases with the increasing Al_2O_3 concentration. The other possibility is that co-doping of Al_2O_3 favors the forming of traps such as oxygen vacancies.

Although we have made some progress in understanding the hole-formation mechanism, there are still many unsolved problems. For example, how the electrons produced by the ionization of Sm^{2+} are captured. This question still remains unclear. In this paper, we mainly study the hole-profiles and the hole-growth dynamics in an Sm^{2+}-doped Al_2O_3–SiO_2 glass. The hole-burning experiments were performed at 300 K, because we expected that more information about the hole-formation could be revealed at room temperature. In addition, the experiment of multi-hole-burning was also performed at that temperature.

2. Experiments

$15Al_2O_3 \cdot 85SiO_2$ (mole ratio) glass containing 5 wt% Sm_2O_3 was prepared by the following process. $Si(OC_2H_5)_4$ was partially hydrolyzed with a mixed solution of H_2O, C_2H_5OH and HCl with a molar ratio of 1:1:0.027 per mol of $Si(OC_2H_5)_4$. After the solution was stirred for 1 h, $Al(OC_4H_9)_3$ was added, followed by refluxing at 800 °C for 5 h; then $SmCl_3 \cdot 5H_2O$, which was ultrasonically dissolved in C_2H_5OH, was mixed with the solution. The resultant solution was hydrolyzed by adding the mixed solution of H_2O, C_2H_5OH, and HCl. After stirring for 15 min, the solution was poured into a polystyrene container with cover, and left at room temperature for 5 days to form a stiff gel. The stiff gel was dried at room temperature for 10 days. The stiff gel was heated in air for 1 h at 800 °C to form glass. The obtained glass has an optical absorption spectrum with sharp lines at 345, 360, 375 and 403 nm, which are all assigned to the Sm^{3+}-ions. To reduce the Sm^{3+}-ions to Sm^{2+}, the glasses were heated at 800 °C under flowing H_2 gas for 100 h. After heating in H_2, the glass became pink, indicating the formation of Sm^{2+}-ions [8]. A glass plate with a thickness of ~1 mm and area of ~1 cm^2 was used as sample.

A pulsed Nd:YAG (yttrium–aluminum-garnet) laser pumped anoimidazole (DCM) dye laser with a repetition frequency of 10 Hz and a band width of 0.1 nm at half-maximum was used for hole-burning within the $^7F_0$–$^5D_0$ spectral line. The burning light focused on the glass with an area of ~0.2–0.5 mm^2. The excitation spectra of $^7F_0$–$^5D_0$ transition were measured before and after burning by scanning the laser while monitoring the fluorescence of the $^5D_0$–$^7F_2$ transition near the peak position. The laser power for reading the holes was attenuated by neutral density filters to be 0.3% of that for hole burning. The experimental setup was drawn as Fig. 1.

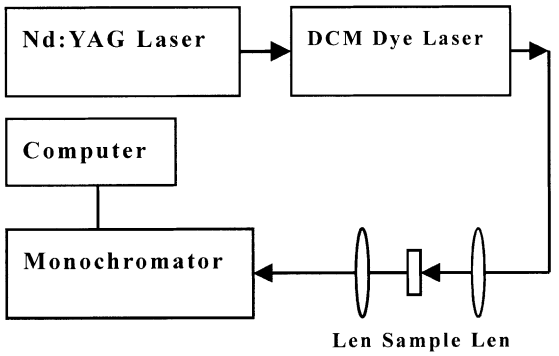

Fig. 1. Experimental setup for the measurement of PSHB.

3. Results and discussion

3.1. Hole-profiles at room temperature

Fig. 2(a) shows the excitation spectra measured before and after hole-burning for different times, and (b) shows the differences of the spectra before and after hole-burning. It is evident that the depth of the hole increases with increasing time, while the width of the hole broadens. Curve fitting indicates that the holes exhibit Lorentz profiles instead of Gaussian ones. The global (homogeneous + inhomogeneous) excitation line of $^7F_0$–$^5D_0$ before hole-burning was well fitted by a Gaussian function. On the other hand, the excitation line after hole-burning was fitted by the difference of a Lorentzian and a Gaussian function. The central wavelength of the excitation line, λ_1 and the hole central wavelength, λ_2 are 683.7 and 684.0 nm, respectively. At room temperature, the laser width is negligible in comparison with the homogeneous line width. Thus we can conclude that the homogeneous line of $^5D_0$–$^7F_0$ is Lorentzian, which is often observed for rare earth ions doped in crystals and has been explained theoretically [17]. The hole-width at half-maximum obtained from the fitting data was plotted as Fig. 3 against the burning time. From the extrapolation of the hole-width in Fig. 3, we obtained the homogeneous line width to be 0.82 nm. On the other hand, the inhomogeneous line width of $^5D_0$–$^7F_0$ was obtained to be 14.4 nm according to Fig. 2. If we assume that the homogeneous line width does not vary with the excitation wavelength, the ratio of inhomogeneous line width to homogeneous line width can be deduced to be 18. This indicates that at most nine separate holes can be burnt at 300 K ($\Gamma_{\text{hole}} = 2\Gamma_{\text{h}}$). In Sm^{2+}-doped halide-earth-metal fluoride crystals, seven distinguished holes were burnt at room temperature [18]. The inhomogeneous line width of the $^7F_0$–$^5D_0$ transition of the glass is broadened greatly in comparison with that of the crystal; however, due to the homogeneous

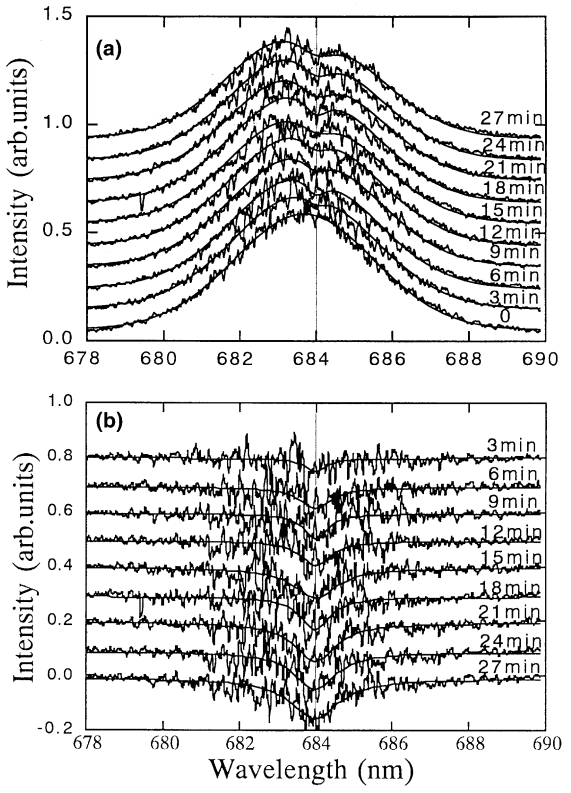

Fig. 2. (a) Hole spectra measured after hole burning with a laser light for different times ($\lambda = 684$ nm, $P = 150$ mW). (b) Differences between the spectra before and after hole-burning. The smooth curves are experimental data and the lines fitting functions.

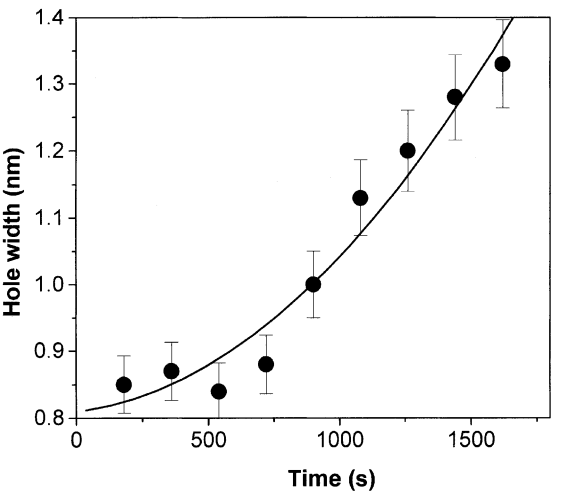

Fig. 3. Hole-width as a function of burning-time. The experimental data are obtained from the Lorentz fitting functions corresponding to Fig. 2.

line width also being broadened, the limitation of storage density is not broken through.

3.2. Multi-hole-burning

The hole-burning at different excitation wavelengths was also performed at 300 K. In the experiment, holes were burnt at wavelengths of 684, 682, 686, 680 and 688 nm in turn. The excitation spectra before and after multi-hole-burning were plotted as Fig. 4. As shown, the first hole burnt at 684 nm was clearly observed. For multi-hole-burning, however, the holes overlapped each other. A broadened hole centered at 684 nm was observed. After burning at the other sites, the depth of the hole at 684 nm did not decrease. This indicated that the burning light at the other sites did not optically refill the hole formed in advance. The traps filled by electrons were not ionized by the photons of the burning light. From this fact, we can conclude that the energy separation between the trap and the conduction band should be larger than 1.8 eV. The result above also means that, although the hole is formed by one photon, the read-out-induced hole refilling can be avoided as in photon-gated PSHB. This property is quite different from that in Sm^{2+}-doped fluoride mixed crystal [19] and favors FDOS.

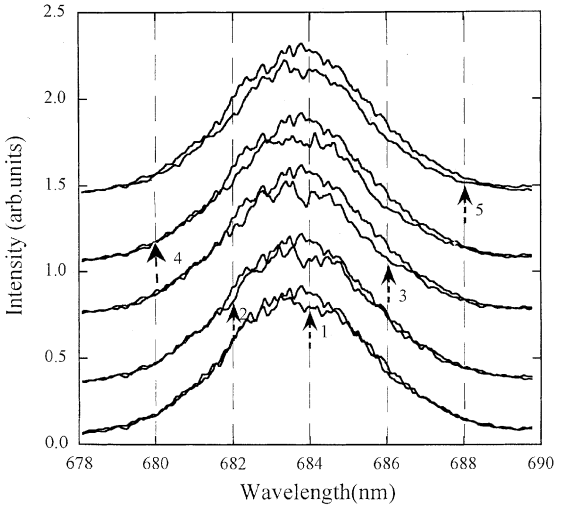

Fig. 4. Excitation spectra after burning at different sites. The holes were burnt at the wavelengths of 684, 682, 686, 680 and 688 nm in turn, as marked in the figure.

3.3. Hole-growth dynamics and data fitting

We assume that the hole-formation mechanism at room temperature in the aluminosilicate glass is the photoionization of Sm^{2+}-ion. The Sm^{2+}-ions offer electrons to the traps by tunneling. In the photoionization mechanism, the oxygen vacancies or the Al^{3+}-ions can be regarded as traps. The build-up of products by hole burning is governed by a rate constant K_t [$K_t = (k_t/k_f)\sigma I$] [20,21], where k_t is a tunneling rate to the ground state (the reciprocal lifetime), σ is the absorption cross-section and I is the photon flux. The normalized concentration of the center M is written by a rate equation

$$dM(t)/dt = -K_t M(t), \tag{1}$$

where $M(0) = 1, M$ can be expressed as an integral function of t

$$M(t) = \exp\left[-\frac{\sigma I}{k_f}\int k_t\,dt\right]. \tag{2}$$

If the rate k_t is independent of burning time, hole-growth data should follow a simple exponential of $M(t) = \exp(-K_t t)$ from the burning equation. Hole product $[H(t) = 1 - M(t)]$ equals $1 - \exp(-K_t t)$. Accordingly, the maximum of hole-depth may approach 100%. Nevertheless, the maximum of hole-depth is less than 25% in the experiments here. If we simply consider the optical saturation effect, the hole production is given as

$$H(t) = q[1 - \exp(-K_t t)], \tag{3}$$

where q is a constant that is satisfied with $0 < q < 1$. We fitted the experimental data with Eq. (2); however, the time development of the hole-depth deviates from such a function.

The non-exponential profile of hole-growth suggests that k_t varies with the hole-burning time. We proposed several simple functions of k_t such as $k_t = k_0/t$ and $k_t = k_0(1 - k_1 t)$ and derived $M(t)$ as a function of t; however, the experimental dynamics deviate from such functions. Then, we fitted the experimental data by some simple functions. Fortunately, the data were well fitted by

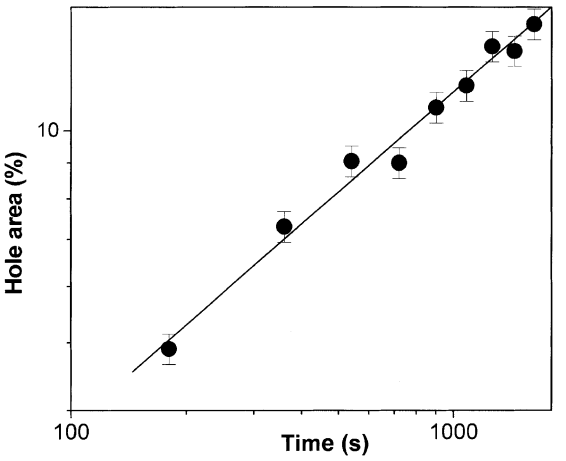

Fig. 5. Normalized hole-area against burning-time ($\lambda = 684$ nm, $P = 150$ mW). The curves are drawn in log–log scale. The dots are experimental data and the lines are several fitting functions.

$$H(t) = \alpha t^{\beta} (\alpha > 0, 0 < \beta < 1). \tag{4}$$

Fig. 5 shows the normalized hole-area against the burning time and the fitting function in the log–log scale. It is evident that Eq. (4) is a better fitting function.

3.4. Laser power dependence of hole-growth dynamics

Fig. 6 shows the experimental hole-depths as a function of burning time pumped with different laser powers and the fitting results with Eq. (4). The fitting parameters, α and β, vary with the laser power density. The variation of α and β with laser power P is listed as Table 1. It is evident that α increases quickly and almost linearly with the increase of laser power of the hole-burning light, indicating that the hole burning is a one-photon process. On the other hand, β increases a little with the increase of laser power, and is always in the range of $0.5 < \beta < 1$. By Eqs. (1) and (4), the hole-growth rate K_t could be derived as

$$K_t = \frac{\alpha\beta t^{\beta-1}}{1 - \alpha t^{\beta}}. \tag{5}$$

We calculated K_t against hole-burning time according to Eqs. (5) and the parameters listed in Table 1, which were drawn as Fig. 7. It is evident

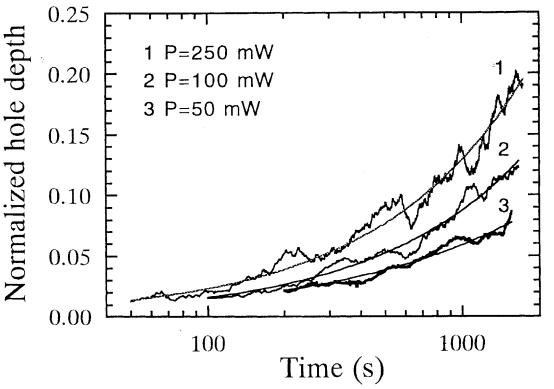

Fig. 6. Hole-growth dynamics pumped with different laser powers. (The fitting function is $H(t) = \alpha t^{\beta}$.)

Table 1
Variation of parameters α and β with the power of burning light

P (mW)	α (10^{-4} s^{-1})	β
50	4.4 ± 0.4	0.71 ± 0.05
100	5.2 ± 0.3	0.74 ± 0.03
250	6.9 ± 0.4	0.76 ± 0.03

that K_t decreases as the burning time increases and as the laser power of burning light decreases.

3.5. Origin of the non-exponential hole-growth

The non-exponential hole-growth was also observed and studied in the $^7F_0$–$^5D_2$ transition

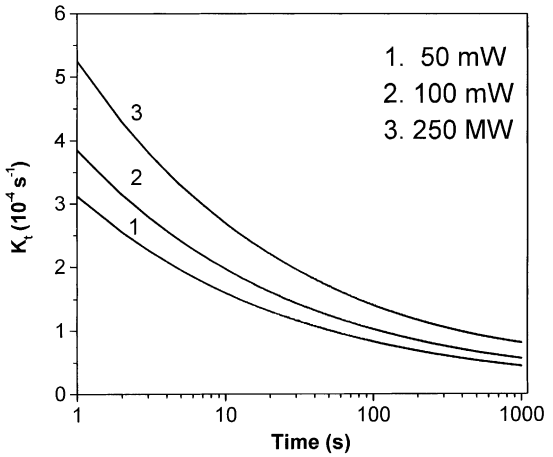

Fig. 7. Hole-growth rate K_t against t. The parameters α and β are chosen according to the fitting results related to Fig. 6.

(560 nm) of Sm^{2+}-doped single crystal, which was attributed to the two paths of hole burning, one-step tunneling in the excited state and two-photon ionization through the conduction band [22]. In our present case, the hole-burning rate constant is proportional to the laser power of burning light, indicating that the spectral hole is formed predominantly by one-photon process. As mentioned above, the optically activated rearrangement of OH bonds surrounding Sm^{2+}-ions does not contribute to PSHB above 200 K because of the weak thermal stability of burnt holes. Therefore, the formation mechanism of spectral hole at room temperature is mainly attributed to the electron tunneling of Sm^{2+}-ions with traps. The non-exponential dynamics are not caused by the formation of a different hole.

We assume that an Sm^{2+} center and the trap nearest to the Sm^{2+}-ion made up of a two-level-system (TLS). TLS with a short distance has a large k_t and tunnels at a short time. TLS with a long distance has a small k_t and tunnels over a long time. If the distance of the TLS is too long, the electron of Sm^{2+} cannot tunnel with the trap. It should be pointed out that the concept of the TLS here deviates from the traditional concept of TLS. In the traditional concept of TLS, the doping ions couple with the TLS in glasses or the other amorphous solids and therefore cause the spectral diffusion of homogeneous line width [23]. In the Sm^{2+}-doped $85Si_2O_3$–$15Al_2O_3$ glass, the ratio of Al_2O_3 to Sm_2O_3 in mol is about 15:1. In the glass network, most of the aluminum ions exist with the valence-state of +3. On the other hand, not all of the Sm^{3+}-ions are reduced to Sm^{2+}. This means, if Al^{3+}-ions act as traps or the forming of one Al^{3+}-ion produces one oxygen vacancy considering charge compensation in the doping of trivalent ions into the SiO_2 glass, the total density of traps would be much larger than that of the Sm^{2+}-ions. In this case, if the interaction length between the Sm^{2+} and the traps is short and the traps tend to gather around Sm^{2+}-ions, hole-depth should approach 100% if the laser power is high enough. However, the result is quite different. Therefore, we can assume that for some of the Sm^{2+}-ions, the distance between the Sm^{2+}-ion and the nearest trap is beyond the interaction range of tunneling in the glass network. These Sm^{2+}-ions do not contribute to the formation of spectral hole.

4. Conclusions

In this paper, we mainly investigated hole-profiles and hole-burning dynamics of Sm^{2+} doped in aluminosilicate glasses at room temperature. We observed that the spectral holes exhibit Lorentz profiles. The hole burned in advance cannot be refilled by the burning-light at the other sites, which favors the FDOS. Hole-growth dynamics can be well fitted by the function of $H(t) = \alpha t^{\beta}$, indicating that the growth rate K_t is not a constant. K_t is deduced as a function of time. It can be concluded that for some of the Sm^{2+}-ions, the distance between the Sm^{2+}-ion and the nearest trap is beyond the interaction range of tunneling in the glass network.

Acknowledgements

This research was supported by One Hundred Talents Project, sponsored by Chinese Academy of Sciences and by a Grant-in-Aid for Scientific Research (No. 09650734) from the Ministry of Education, Science, and Culture of Japan.

References

[1] W.E. Moerner (Ed.), Persistent Spectral Hole Burning: Science and Applications, Springer, Berlin, 1998.
[2] R. Jaaniso, H. Bill, Europhys. Lett. 16 (1991) 549.
[3] K. Holloday, C. Wei, M. Croci, U.P. Wild, J. Lumin. 53 (1992) 227.
[4] J. Zhang, S. Huang, J. Yu, Opt. Lett. 17 (1992) 149.
[5] M. Nogami, Y. Abe, Phys. Rev. B 56 (1997) 182.
[6] K. Hirao, S. Todorori, D.H. Cho, N. Soga, Opt. Lett. 18 (1993) 1586.
[7] A. Kurita, S. Todorori, D.H. Cho, N. Soga, Opt. Lett. 19 (1994) 314.
[8] M. Nogami, Y. Abe, Appl. Phys. Lett. 64 (1994) 1227.
[9] M. Nogami, Y. Abe, K. Hirao, D.H. Cho, Appl. Phys. Lett. 66 (1995) 2952.
[10] K. Fujita, K. Hirao, N. Soga, Opt. Lett. 23 (1998) 543.

[11] M. Nogami, T. Hayakawa, J. Non-Cryst. Solids 241 (1998) 98.
[12] M. Nogami, T. Umehara, T. Hayakawa, Phys. Rev. B 58 (1998) 6166.
[13] M. Nogami, T. Hayakawa, Phys. Rev. B 56 (1997) 14235.
[14] M. Nogami, T. Nagakula, T. Hayakawa, T. Sakai, Chem. Mater. 10 (1998) 3991.
[15] H. Song, T. Hayakawa, M. Nogami, Phys. Rev. B 59 (1999) 11760.
[16] H. Song, T. Hayakawa, M. Nogami, Opt. Commun. 165 (1999) 49.
[17] A.M. Stoneham, Rev. Mod. Phys. 41 (1969) 82.
[18] R. Jaaniso, H. Bill, J. Lumin. 64 (1995) 173.
[19] H. Song, J. Zhang, S. Huang, J. Yu, Solid State Commun. 99 (1996) 759.
[20] R. Jankowiak, R. Richert, H. Bassler, J. Phys. Chem. 89 (1985) 4569.
[21] T. Okuno, T. Suemoto, Phys. Rev. B 59 (1999) 9078.
[22] J. Zhang, H. Song, Y. Zhao, M. Tian, S. Huang, J. Yu, J. Lumin. 64 (1995) 207.
[23] K.A. Littau, Y.S. Bai, M.D. Fayer, J. Chem. Phys. 92 (1990) 4145.